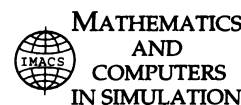




ELSEVIER

Mathematics and Computers in Simulation 55 (2001) 329–340



www.elsevier.nl/locate/matcom

Spatiotemporal chaos in spatially extended systems

David Cai*, David W. McLaughlin, Jalal Shatah

Courant Institute of Mathematical Sciences, New York University, New York, NY 10012, USA

Received 15 December 1999; accepted 4 May 2000

Abstract

To address finite-size effects in the use of the decay mutual information to characterize spatiotemporal chaotic dynamics, we modify the dispersion of the nonlinear Schrödinger equation to obtain a model system for which the number of unstable modes remains *fixed* while the domain size increases. Our numerical study of the model system clearly establishes that spatiotemporal chaos arises in the presence of only two unstable modes. In this spatially extended system, the spatiotemporal chaos is characterized by chaotic dynamics in time and by an exponential decay in space of mutual information, with the decay rate becoming system-size independent in the large system-size limit. © 2001 IMACS. Published by Elsevier Science B.V. All rights reserved.

Keywords: Spatiotemporal chaos; Non-linear Schrödinger equation; Partial differential equations (PDE)

1. Introduction

The concept of deterministic chaos in finite dimensional systems has been extended to spatially extended systems described by partial differential equations (PDE), which are infinite dimensional dynamical systems with spatial structures. The existence of *temporal chaos* in nearly integrable systems, such as perturbed nonlinear Schrödinger (NLS) equations, is well established and is linked to linear instabilities in integrable soliton dynamics [1]. In these systems, temporal chaos arises from underlying hyperbolic structures which can result in homoclinic orbits for the integrable PDEs. These are the sources of sensitivity and can, when perturbed, generate chaotic responses. Temporal chaos in perturbed NLS constitutes spatially regular, coherent localized waves which evolve chaotically in time. For example, under even, periodic boundary conditions, in small spatial domains with only one instability and only one solitary wave, a “soliton” jumps chaotically between the center and edge locations of a periodic system. The regular spatial profile can be described by a strong statistical correlation between the time series at location x , of the temporally chaotic wave $\psi(x, t)$, and the time series of wave $\psi(y, t)$ at y , $y \neq x$.

* Corresponding author.

As demonstrated in [2–5], the hyperbolic structure in NLS gives rise not only to temporal chaos, but also to *spatiotemporal* chaos. Intuitively, spatiotemporal chaos arises from the following scenario: by enlarging the domain size and relaxing even symmetry, one introduces increasing number of instabilities into the system, hence increasing number of distinct classes of spatial excitations in the form of solitary waves, standing waves, waves traveling to the left and right, bound states, etc. Therefore, introduction of more instabilities creates more and more spatially complex structures in the system. Statistically, in addition to the loss of information in time as characterized by temporal chaos, one would expect this “spatial complexity” to decorrelate the system, with the time series of waves, $\psi(x, t)$ and $\psi(y, t)$, becoming independent as the distance from x to y increases, signifying loss of information over space.

There have been many definitions of spatiotemporal chaos, emphasizing various chaotic aspects of dispersive waves in space [6]. We have used a “working definition” which includes two points: (i) a temporally chaotic wave $\psi(x, t)$; (ii) for which the time series $\{\psi(x, t), \forall t\}$ and $\{\psi(y, t), \forall t\}$ become statistically independent as the distance from x to y increases. Furthermore, we have used vanishing mutual information $\mathcal{I}(x, y)$ to quantify this statistical independence, which is a stronger measure of statistical independence than the commonly used two-point correlation function, since vanishing mutual information is a necessary and sufficient condition for statistical independence. For dispersive waves, the mutual information between two point x and y can be defined as

$$\mathcal{I}(x, y) = \int du dv p_{x,y}(u, v) \log \frac{p_{x,y}(u, v)}{p_x(u)p_y(v)}, \quad (1)$$

where the distributions $p_{x,y}(u, v)$, $p_x(u)$ and $p_y(v)$ are generated through time series $\{\psi(x, t), \forall t\}$ and $\{\psi(y, t), \forall t\}$. Intuitively, $p_{x,y}(\psi(x), \psi(y)) d\psi(x) d\psi(y)$ is the fraction of time that both $\psi(x, \cdot) \in (\psi(x), \psi(x) + d\psi(x))$ and $\psi(y, \cdot) \in (\psi(y), \psi(y) + d\psi(y))$ simultaneously, and $p_x(\psi) d\psi$ is the fraction of time that $\psi(x, \cdot) \in (\psi, \psi + d\psi)$, etc. In terms of this mutual information, the working definition used in [2–5] can be summarized as follows:

A wave $\psi(x, t)$ is spatiotemporal chaotic if

1. $\psi(x, t)$ is a temporally chaotic orbit (e.g. as characterized by bounded, not asymptotically periodic orbits with positive Lyapunov exponents);
2. the mutual information between two spatial points, $\mathcal{I}(x, y)$, decays exponentially in space as $|x - y| \rightarrow \infty$.

Using this definition of spatiotemporal chaos, we have shown that spatiotemporal chaos indeed is observed in the driven, damped NLS equation

$$i\psi_t + \psi_{xx} + 2|\psi|^2\psi = -i\alpha\psi + \Gamma e^{i(\omega t + \gamma)} \quad (2)$$

with periodic boundary conditions, $\psi(x + L) = \psi(x)$, where L is the system length, ω and γ the driving frequency and phase, respectively. The damping coefficient α and the driving strength Γ are small parameters. Furthermore, it was found that the onset of spatiotemporal chaos can be induced by a very small number of instabilities — *two* for the system (2). For the NLS system (2), the number of instabilities is associated with the size of domain. For example, in the studies of spatiotemporal chaos [2–5], data very close to the trivial x -independent solution of the unperturbed NLS

$$\psi(x, t) = A \exp[-i(2A^2t + \sigma)], \quad (3)$$

was initialized (here A is the amplitude of the wave and σ the phase). This plane wave (3) is linearly unstable with the number of instabilities determined by $0 < k^2 < 4A^2$, where $k = 2\pi m/L$ is the wavenumber of the linearized wave and m is an integer. One can see that the number of unstable modes scales linearly with the size L of the periodic spatial domain.

In the numerical studies [2–5], the mutual information of a temporally chaotic state with one spatially regular solitary wave, associated with one instability, is nonvanishing. Whereas, the mutual information of waves associated with more than one instability decays over space, hence the *onset* of spatiotemporal chaos. In order to use the working definition of spatiotemporal chaos, to make precise the statement that the spatiotemporal chaos indeed arises for a *small* number of instabilities, one has to demonstrate that, for a *fixed* small number of instabilities, there is an exponential decay of mutual information in space. To ascertain the exponential decay as $|x - y| \rightarrow \infty$, one needs an infinite spatial domain — or, at least, a sufficiently large spatial domain that finite-size effects can be eliminated. However, as we discussed above, increasing the domain size for the perturbed NLS, also simultaneously increases the number of linearly unstable modes. Therefore, to ensure that only two instabilities are required for spatiotemporal chaos, one must find a dispersive wave system such that there is an exponential decay of mutual information for a fixed (small) number of linearly unstable modes while simultaneously the system size is increased. This is the issue that we will study in this paper.

We note that a similar question has also been investigated for a modified Kuramoto–Sivashinsky equation [7], in which the usual (k^2 – k^4)-dispersion of the Kuramoto–Sivashinsky equation is replaced by a nonlocal linear operator with two linearly unstable modes. In contrast to our decaying mutual information characterization of spatial chaos, spatial complexity is characterized in [7] by the topological entropy of a symbolic language associated with *stationary* solutions in space. There, the question of how to dynamically visit all these stationary states in time remains to be fully addressed [6,7]. In our approach, we will follow a similar construction for the linear, dispersive operator. However, we will stress both temporal and spatial chaotic aspects of dynamics.

To seek a candidate system which possesses the exponential decay of mutual information for a fixed small number of instabilities with the increasing size of system, the approach we take is to keep the nonlinearity of the NLS (2), and to modify the dispersion such that plane waves are unstable to a (small) number of instabilities, which remains constant as the system size increases. As a result, the modified NLS is an integro-differential equation in x -space and the linear operator becomes nonlocal. For this modified equation, we numerically study the behavior of the mutual information and two-point correlation functions. As reported below, when there is only one instability, the dispersive wave is statistically well correlated over the whole domain. In contrast, when there are two instabilities, the dispersive wave exhibits an exponential decay of mutual information in space. The decay rate becomes independent of system size as the domain size increases. Our numerical study clearly establishes that the dynamics of system exhibits spatiotemporal chaos for only two unstable modes. We will also study detailed aspects of the dynamics, such as the relation between spatial decay lengths determined by the two-point correlation function and those determined by the mutual information and its implication for Gaussianity of the joint distribution of waves between two distinct spatial points.

In Section 2, we will carry out the modification of the dispersion to obtain our model system and discuss the linear stability of the system. In Section 3, we present the numerical method used for our numerical study. In Section 4, we report our numerical results and discuss various aspects of the dynamics. We conclude the paper with Section 5.

2. The model

The strategy, we employ to construct a system with a fixed number of unstable modes is to replace the linear operator for the dispersive part of NLS, while leaving the nonlinear part intact. In Fourier representation, the unperturbed NLS on the real line can be written as

$$i\dot{a}_k = k^2 a_k - \frac{2}{(2\pi)^2} \int a_{k_1} a_{k_2} a_{k_3}^* \delta(k + k_3 - k_1 - k_2) dk_1 dk_2 dk_3.$$

We replace the dispersion k^2 with the following dispersion

$$D(k) = \begin{cases} k_1^2 \delta(|k| - k_1) + \lambda k_2^2 \delta(|k| - k_2), & \text{for } |k| < k_c, \\ k^2, & \text{for } |k| \geq k_c, \end{cases}$$

where δ denotes the Dirac delta function, k_1 and k_2 the fixed wavenumbers, $k_1 < k_2 < k_c$, and above the threshold k_c is the usual dispersion k^2 . The parameter $\lambda = 0$ corresponds to one-mode truncation and $\lambda = 1$ to two-mode truncation (see below). This modification of dispersion yields a new equation of motion:

$$i\dot{a}_k = D(k) a_k - \frac{2}{(2\pi)^2} \int a_{k_1} a_{k_2} a_{k_3}^* \delta(k + k_3 - k_1 - k_2) dk_1 dk_2 dk_3, \quad (4)$$

which is an integro-differential equation in x -space. Here the linear operator is no longer local. There are at least two conserved quantities, namely, energy \mathcal{H} and norm \mathcal{N}

$$\mathcal{H} = \int D(k) a_k a_k^* - \frac{2}{(2\pi)^2} \int a_k^* a_{k_1}^* a_{k_2} a_{k_3} \delta(k + k_1 - k_2 - k_3) dk dk_1 dk_2 dk_3,$$

$$\mathcal{N} = \int a_k a_k^* dk.$$

For a periodic domain of size L , the new dispersion is simply

$$D_L(k) = \begin{cases} k_1^2 \delta_{|k|, k_1} + \lambda k_2^2 \delta_{|k|, k_2}, & \text{for } |k| < k_c, \\ k^2, & \text{for } |k| \geq k_c, \end{cases} \quad (5)$$

where $k = 2\pi m/L$, m being an integer. In this case, the values of k_1 and k_2 have to be chosen to be compatible with the discreteness of wavenumbers, i.e. for some L , $k_1 = 2\pi m_1/L$ and $k_2 = 2\pi m_2/L$ for some integer m_1 and m_2 . Once these values are chosen, the limit of increasing large L is taken at a discrete set of L -values, i.e. qL with q being integer, in order for us to be able to keep k_1 and k_2 fixed, regardless of the domain size.

For this new system in a periodic domain, the trivial x -independent plane wave solution is the same as Eq. (3) with the following Fourier representation

$$a_k^{\text{plane}}(t) = AL \exp[i(2A^2 t + \sigma)] \delta_{k,0}.$$

If there is a small perturbation around $a_k^{\text{plane}}(t)$

$$a_k = a_k^{\text{plane}}(t) + \epsilon_k(t) \exp[i(2A^2 t + \sigma)],$$

for

$$\epsilon_k(t) = \eta_k \exp(i\omega_k t),$$

a simple linear stability analysis leads to

$$\omega_k^2 = D_L(k) (D_L(k) - 4A^2). \tag{6}$$

Eq. (6) shows that if we choose the value of A such that $k_2^2 < 4A^2 < k_c^2$, then (for $\lambda = 1$) there are only two linearly unstable modes at k_1 and k_2 (there is only one linearly unstable mode at k_1 , if $\lambda = 0$). In the following, we will refer to the case of $\lambda = 0$ as the one-mode truncation model and the case of $\lambda = 1$ as the two-mode truncation model.

When perturbations of driving and damping similar to those in Eq. (2) are added, we have the following equation:

$$i\dot{a}_k = D_L(k)a_k - \frac{2}{L^2} \sum_{p,q} a_p a_q a_{p+q-k}^* - i\alpha a_k + L\Gamma e^{i(\omega t + \gamma)} \delta_{k,0} \tag{7}$$

in a periodic domain with size L . In this model, we can address the question raised above, i.e. whether the two-mode instability will give rise to exponentially decaying mutual information in space. This model allows us to keep k_1 and k_2 fixed while enlarging the domain size L to eliminate finite-size effects. With the increasing L , if the mutual information decays in space with decay rate becoming independent of L , then, clearly, this model is an example of spatiotemporal chaos with only two instabilities. We will investigate this question numerically.

3. Numerical method

The structure of Eq. (7) suggests that it is very natural to use the integrating factor method to remove stiffness in the problem [8] and to employ a fast Fourier transform (FFT) pseudospectral method to deal with the nonlinearity. This is achieved via a new set of variables $v_k(t)$ which satisfy

$$v_k(t) \equiv \left[a_k(t) - \frac{L\Gamma\delta_{k,0}}{i\theta_k - \omega} e^{i(\omega t + \gamma)} \right] e^{\theta_k t}, \tag{8}$$

where $\theta_k = iD_L(k) + \alpha$ and

$$i\dot{v}_k = -2F_+\{|F_-\{a_k\}|^2 F_-\{a_k\}\} e^{\theta_k t}, \tag{9}$$

$$a_k = v_k(t) e^{-\theta_k t} + \frac{L\Gamma\delta_{k,0}}{i\theta_k - \omega} e^{i(\omega t + \gamma)}. \tag{10}$$

Here F_+ and F_- stand for the Fourier and inverse Fourier transforms. A fourth-order adaptive stepsize Runge–Kutta integrator is used for time integration for Eq. (9). In this numerical method, the modified dispersion (5) does not introduce any additional numerical complications — if a direct x -representation of $\psi(x)$ were used, one would have to solve an integral-differential equation in x -space. Total numbers of modes $N = 256, 512,$ and 1024 were used for various spatial sizes. The unstable mode wavenumbers $k_1 = 0.409, k_2 = 0.818,$ and the threshold wavenumber $k_c = 1.636$ were chosen in all runs. The damping coefficient is $\alpha = 10^{-6}$. The driving strength and frequency is $\Gamma = 5 \times 10^{-4}$ and $\omega = 1,$ respectively.

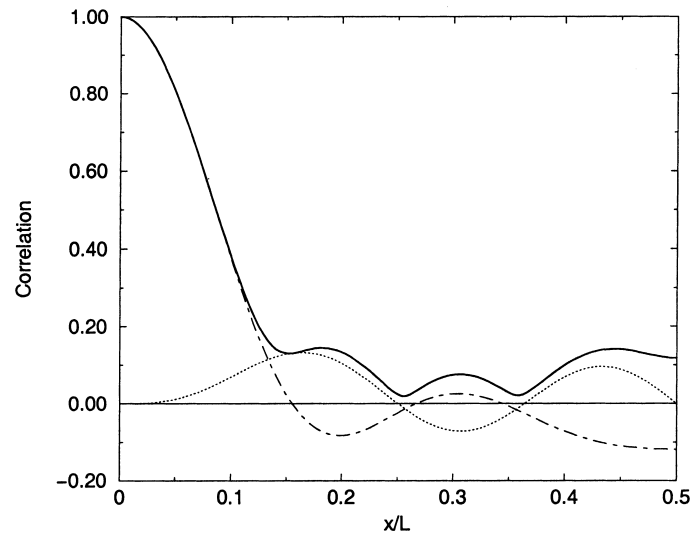


Fig. 1. Correlation function for one-mode truncation. Solid line: $|C(x)|$; dot-dashed line: $\text{Re } C(x)$; dotted-line: $\text{Im } C(x)$. They are all normalized by $C(0)$; $L = 15.36$.

4. Spatiotemporal chaos

Numerically, we compute both the mutual information $\mathcal{I}(x - y)$ and the two-point correlation function

$$C(x) = \lim_{T \rightarrow \infty} \frac{1}{LT} \int_0^T \int_0^L \psi(y, t) \psi^*(y + x, t) dt dy, \quad (11)$$

where we have assumed spatial translational symmetry. We will use $\langle \dots \rangle$ to denote the average over space and time. Note that $\langle \psi(\cdot, \cdot) \rangle = 0$, which is verified numerically. In all runs, we wait for the system to settle down, remove an initial transient and, then, use only the remaining solutions for the computation of these statistical measures. Our results show that, for all system sizes L studied, the correlation function does not vanish across the system for the case of the one-mode truncation (Fig. 1). This is intuitively consistent with the corresponding evolution of the wave $\psi(x, t)$ observed for the one-mode truncation as shown in Fig. 2, which should be contrasted with Fig. 3 for the two-mode truncation. Clearly, the spatial profiles exhibit relatively regular patterns for the one-mode truncation compared with those of the two-mode truncation, which are far more varied and “violent”. Note that the two spatial profiles in Figs. 2 and 3 are shown over the same spatial range and for the same time duration. The temporal chaotic nature of these evolutions are diagnosed numerically by positive Lyapunov exponents, Poincaré sections, broad band power spectra, etc. [1]. For example, the largest positive Lyapunov exponents are +0.11 and +0.34 for the one-mode and two-mode truncations (as shown in Figs. 2 and 3), respectively. Corresponding to the evolution of dynamics of the one-mode truncation shown in Fig. 2, the surface cross section $\{\text{Re } a_{k=0}(t), \text{Im } a_{k=0}(t), \forall t\}$ is shown in Fig. 4, and the Fourier power spectrum is in Fig. 5, which has a very broad spectral band.

The “violent” wave evolution of the two-mode truncation should, intuitively, give rise to statistically less dependent time series of $\psi(x, t)$ and $\psi(y, t)$ for ever increasing separation between x and y . This is

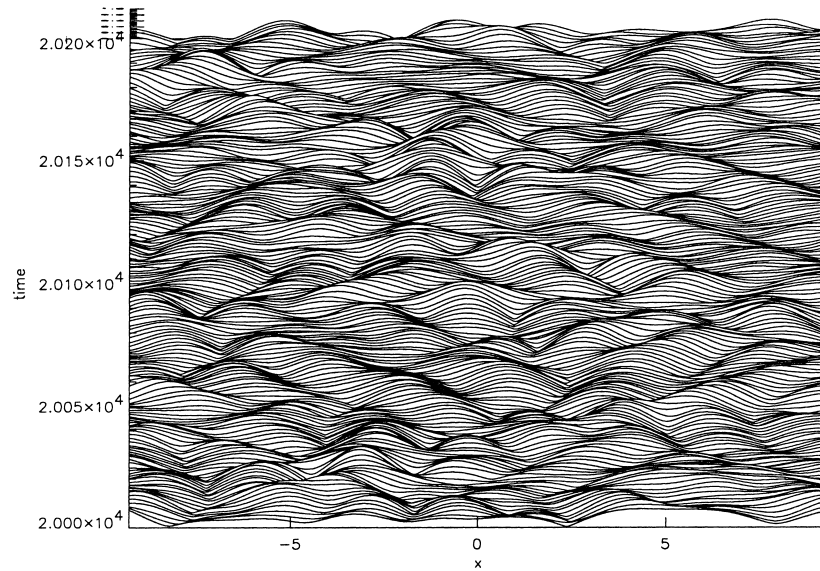


Fig. 2. Evolution of the system (7) with one-mode truncation ($\lambda = 0$). Plotted here is $|\psi(x, t)|$. Only a portion of the system ($L = 30.72$) is shown.

indeed the case: the mutual information for this case displays a clear exponential decay in space as shown in Fig. 6. Fig. 6 displays the decay of mutual information for three different system sizes, $L = 15.36$, 30.72 and 61.44 . For the small size, $L = 15.36$, there is a slight deviation from the exponential decay of the larger sizes, signifying a finite-size effect. However as we increase the system size from $L = 30.72$

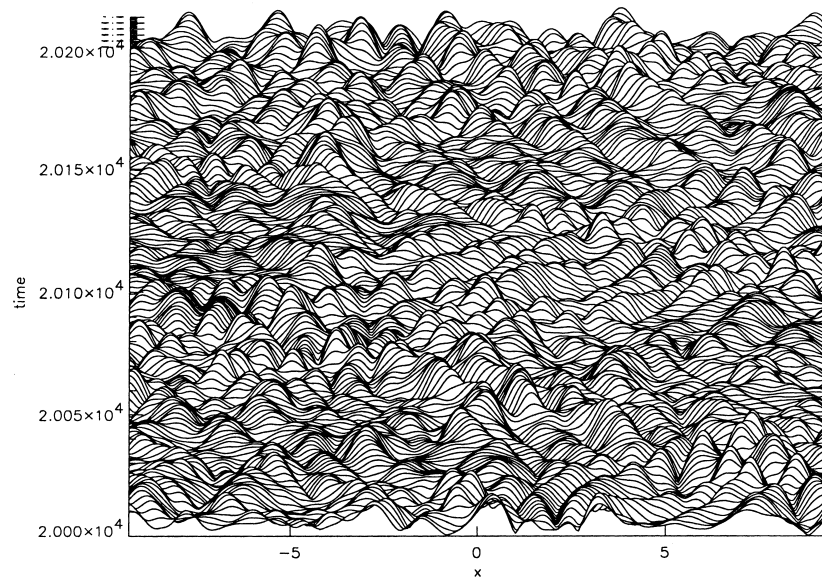


Fig. 3. Evolution of the system (7) with two-mode truncation ($\lambda = 1$). Plotted here is $|\psi(x, t)|$. Only a portion of the system ($L = 30.72$) is shown.

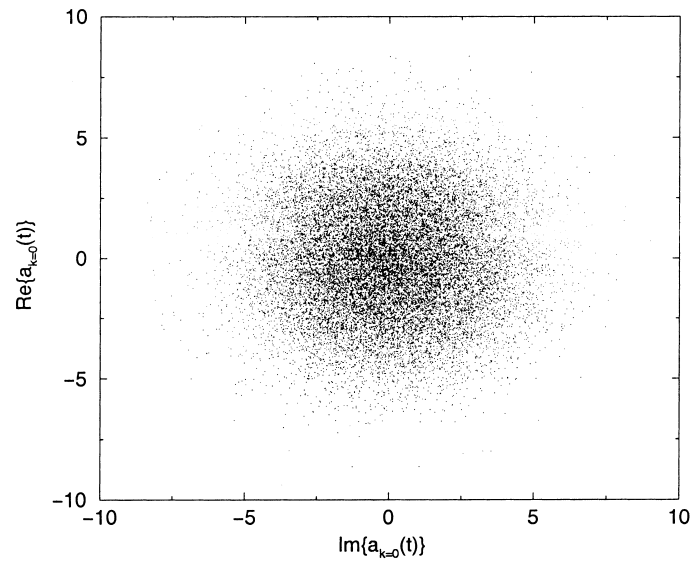


Fig. 4. Temporal chaos: the surface cross-section $\{\text{Re } a_{k=0}(t), \text{Im } a_{k=0}(t), \forall t\}$ corresponding to the evolution of $\psi(x, t)$ (Fig. 2).

to 61.44, their mutual information coincide with each other (as the data symbols almost lie top of each other in Fig. 6 for these two cases). The best fit yields an exponential form

$$\mathcal{I} \sim \exp\left(-\frac{x}{\xi_{\mathcal{I}}}\right) \quad (12)$$

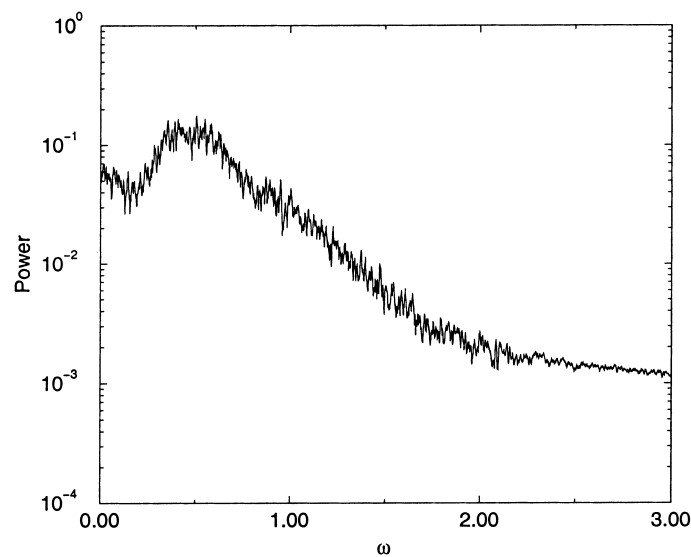


Fig. 5. Temporal chaos: broad band Fourier power spectrum of $a_{k=0}(t)$ corresponding to the evolution of $\psi(x, t)$ in Fig. 2.

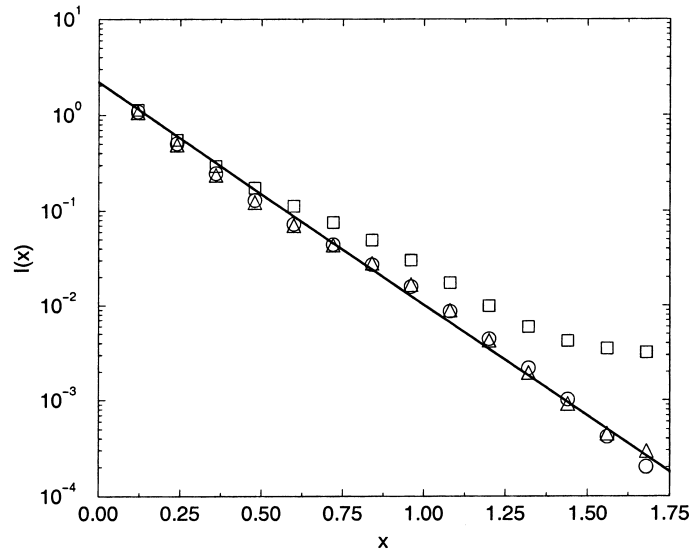


Fig. 6. Decay of mutual information in space for different periodic spatial domain size L . Squares: $L = 15.36$; triangles: $L = 30.72$; circles: $L = 61.44$. The straight line is an exponential fit: $\mathcal{I} \sim \exp(-x/0.186)$.

with $\xi_{\mathcal{I}} = 0.186$. The numerical result here demonstrates that, as L becomes larger and larger, there is an exponential decay of mutual information for the two-mode truncation and the exponential decay rate becomes L -independent. This provides a clear example of spatiotemporal chaos in the presence of only two unstable modes — waves at large separations become statistically independent, leading to the loss of information in space as characterized by the decaying mutual information.

Finally, we discuss the property of the distribution $P_{x,y} \equiv p_{x,y}(\psi(x), \psi(y))$, which underlies these mutual information and correlation function measurements. For a Gaussian distribution, obviously, the mutual information is determined by the two-point correlation function [3,5]. As shown in [3,5] in the Gaussian case, the mutual information decay length $\xi_{\mathcal{I}}$ is related to the correlation decay length ξ_C by

$$\xi_C = 2\xi_{\mathcal{I}}. \tag{13}$$

For the two-mode truncation, the two-point correlation (11) also exhibits an exponential decay as shown in Fig. 7. The measured decay length is $\xi_C = 0.383$. Note that the ratio of $\xi_C/\xi_{\mathcal{I}}$ is 2.06, there being only about 3% deviation from the exact factor 2 of a Gaussian distribution. This approximate relation has also been observed for many spatiotemporal chaotic systems [9,10]. We point out that this approximate relation only indicates that the distribution $P_{x,y} = p_{x,y}(\psi(x), \psi(y))$ may be nearly Gaussian. Fig. 8 is a plot of our numerical measurement of kurtosis K_{31} for the distribution $P_{x,y}$ in the case of the two-mode truncation. K_{31} is defined as follows:

$$K_{31}(x - y) \equiv \frac{\langle R^3(x)R(y) \rangle - 3\langle R(x)R(y) \rangle \langle R^2(x) \rangle}{\langle R^2(x) \rangle \langle R^2(y) \rangle}, \tag{14}$$

where $R(x) \equiv \text{Re } \psi(x)$ and $R(y) \equiv \text{Re } \psi(y)$. (In Eq. (14), it is implicitly assumed that $\langle R(x) \rangle = 0$, which is verified numerically.) For a Gaussian distribution, $K_{31} \equiv 0$. Note that we can obtain the exponential

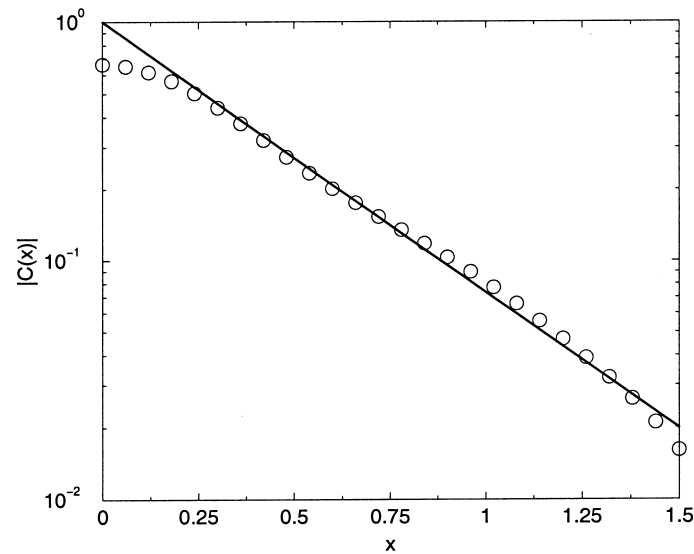


Fig. 7. Correlation function $|C(x)|$ for two-mode truncation; $L = 61.44$. The straight line is an exponential fit: $|C(x)| \sim \exp(-x/0.383)$.

decay of the mutual information or correlation function over the range of separations x even for $x \lesssim 1.75$. In this range of separations, Fig. 8 clearly shows that $p_{x,y}(\psi(x), \psi(y))$ is not Gaussian. It is also important to note that the decay of $K_{31}(x - y)$ for large separations does not necessarily indicate that $P_{x,y}$ becomes more Gaussian as the distance $|x - y|$ increases, since K_{31} can vanish as a consequence of

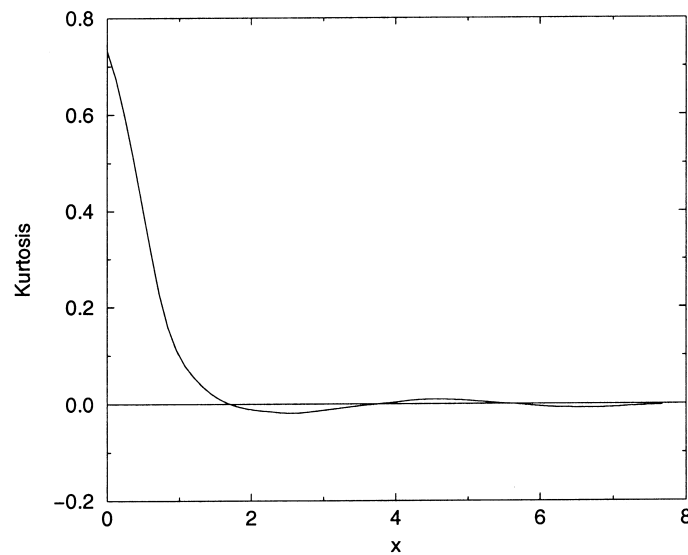


Fig. 8. Kurtosis $K_{31}(x)$ for the distribution $p_{x,y}(\psi(x), \psi(y))$, $y = 0$; $L = 61.44$.

statistical independence between $R(x)$ and $R(y)$, which may not possess a Gaussian distribution between themselves. Due to spatial translational symmetry, $K_{31}(x - y)$ is independent of y . Although in Fig. 8, $y = 0$ is chosen, $K_{31}(x - y)$ does exhibit the same behavior for any y in our numerical measurements. Finally, we mention that similar results also hold for the kurtosis K_{22} (not shown), which is

$$K_{22}(x - y) \equiv \frac{\langle R^2(x)R^2(y) \rangle - 2\langle R(x)R(y) \rangle^2 - \langle R^2(x) \rangle \langle R^2(y) \rangle}{\langle R^2(x) \rangle \langle R^2(y) \rangle}. \quad (15)$$

5. Conclusion

Chaotic nature of dispersive wave turbulence is central to the understanding of nonlinear dispersive waves. The statistical properties of spatial structures over long times can describe whether spatial information is lost or not over large distances. Spatiotemporal chaos arises when waves $\psi(x, t)$ and $\psi(y, t)$ become statistically independent over large separations $|x - y| \rightarrow \infty$. We have demonstrated how to use the decay of mutual information to capture this statistical increasing independence of waves over separations. In our earlier works [2–4], the mutual information measure did capture the *onset* of spatiotemporal chaos in a perturbed NLS with only *two* instabilities. However, as we mentioned above, in the case of the NLS, the number of unstable modes scales linearly with the periodic domain size. Hence, for the perturbed NLS, there is a possible difficulty of finite-size effects in asserting an exponential decay of mutual information over large separations for a small number of instabilities. In the present work, to address the issue of finite-size effects, we use a modified dispersion to obtain a model system which enables us to keep the number of unstable modes *fixed* while the domain size L increases. The results of our numerical study of this model system demonstrate that (1) the dynamics exhibits spatiotemporal chaos as measured by an exponential decay of mutual information in space, in the presence of only two unstable modes, with the decay rate becoming L -independent in the large L limit; (2) there is a statistical correlation over the entire system, when there is only one unstable mode. The temporal dynamics of the both cases is chaotic. This spatially extended model system provides a further example of spatiotemporal chaos which arises from a very small number of instabilities, in contrast to the common belief that spatiotemporal chaos requires systems with many unstable modes [6,11–13].

Acknowledgements

David Cai is supported in part by the Joseph and Hebert Keller Instructorship at New York University, New York and in part by a Sloan Foundation Grant no.96-3-1. David McLaughlin is supported in part by a Sloan Foundation Grant no.96-3-1, AFOSR-49620-98, and NSF DMS-9971813. Jalal Shatah is supported by NSF DMS-9803121.

References

- [1] D.W. McLaughlin, E.A. Overman, Whiskered tori for integral PDEs and chaotic behavior in near integrable pdes, *Surveys Appl. Math.* 1 (1995) 83.
- [2] D. Cai, D.W. McLaughlin, J. Shatah, Spatiotemporal chaos and effective stochastic dynamics for a near integrable nonlinear system, *Phys. Lett. A* 253 (1999) 280.

- [3] D. Cai, D.W. McLaughlin, K.T.R. McLaughlin, The nonlinear Schrödinger equation as both a PDE and a dynamical system, *Handbook in Dynamical Systems*, 1999.
- [4] D. Cai, D.W. McLaughlin, Chaotic and turbulent behavior of unstable 1-D nonlinear dispersive waves, *J. Math. Phys.* 41 (2000) 4125.
- [5] D. Cai, D.W. McLaughlin, J. Shatah, Spatiotemporal chaos for perturbed NLS equations, *J. Nonlinear Sci.* (preprint).
- [6] M. Cross, P. Hohenberg, Pattern formation outside of equilibrium, *Rev. Mod. Phys.* 65 (1993) 851.
- [7] G. Goren, J.P. Eckmann, I. Procaccia, Scenario for the onset of space-time chaos, *Phys. Rev. E* 57 (1998) 4106.
- [8] T.Y. Hou, J.S. Lowengrub, M. Shelley, Removing the stiffness from interfacial flows with surface tension, *J. Comp. Phys.* 114 (1994) 312.
- [9] C.S. O'Hern, D.A. Egolf, H.S. Greenside, Lyapunov spectral analysis of a nonequilibrium Ising-like transition, *Phys. Rev. E* 53 (1996) 3374.
- [10] R.W. Wittenberg, Local dynamics and spatiotemporal chaos — the Kuramoto–Sivashinsky equations: a case study, Ph.D. thesis, Princeton University Press, Princeton, NJ, 1998.
- [11] D.A. Egolf, H.S. Greenside, Characterization of the transition from defect to phase turbulence, *Phys. Rev. Lett.* 74 (1995) 1751.
- [12] K. Sneppen, J. Krug, M.H. Jensen, C. Jayaprakash, T. Bohr, Dynamic scaling and crossover analysis for the Kuramoto–Sivashinsky equation, *Phys. Rev. A* 46 (1992) 7351.
- [13] S. Zaleski, A stochastic model for the large scale dynamics of some fluctuating interfaces, *Phys. D* 34 (1989) 427.